

Formation of stable and reproducible low resistivity and high carrier concentration p-type ZnO doped at high pressure with Sb

J. M. Qin, B. Yao, Y. Yan, J. Y. Zhang, X. P. Jia et al.

Citation: *Appl. Phys. Lett.* **95**, 022101 (2009); doi: 10.1063/1.3153515

View online: <http://dx.doi.org/10.1063/1.3153515>

View Table of Contents: <http://apl.aip.org/resource/1/APPLAB/v95/i2>

Published by the [American Institute of Physics](#).

Related Articles

Phonon-limited electron mobility in graphene calculated using tight-binding Bloch waves

J. Appl. Phys. **112**, 053702 (2012)

Robust mesoscopic fluctuations in disordered graphene

Appl. Phys. Lett. **101**, 093110 (2012)

Time-of-flight mobility of charge carriers in position-dependent electric field between coplanar electrodes

APL: Org. Electron. Photonics **5**, 194 (2012)

Time-of-flight mobility of charge carriers in position-dependent electric field between coplanar electrodes

Appl. Phys. Lett. **101**, 093304 (2012)

A transient electron transport analysis of bulk wurtzite zinc oxide

J. Appl. Phys. **112**, 033720 (2012)

Additional information on *Appl. Phys. Lett.*

Journal Homepage: <http://apl.aip.org/>

Journal Information: http://apl.aip.org/about/about_the_journal

Top downloads: http://apl.aip.org/features/most_downloaded

Information for Authors: <http://apl.aip.org/authors>

ADVERTISEMENT



HAVE YOU HEARD?

Employers hiring scientists
and engineers trust
physicstodayJOBS

<http://careers.physicstoday.org/post.cfm>



Formation of stable and reproducible low resistivity and high carrier concentration *p*-type ZnO doped at high pressure with Sb

J. M. Qin,^{1,2} B. Yao,^{1,3,a)} Y. Yan,³ J. Y. Zhang,¹ X. P. Jia,³ Z. Z. Zhang,¹ B. H. Li,¹
C. X. Shan,¹ and D. Z. Shen¹

¹Laboratory of Excited State Processes, Changchun Institute of Optics, Fine Mechanics and Physics,
Chinese Academy of Sciences, Changchun 130033, People's Republic of China

²Inner Mongolia University for the Nationalities, Tongliao 028043, People's Republic of China

³Department of Physics and State Key Lab Superhard Material, Jilin University, Changchun 130023,
People's Republic of China

(Received 3 February 2009; accepted 22 May 2009; published online 13 July 2009)

Stable *p*-type Sb-doped ZnO (ZnO:Sb) was fabricated reproducibly by sintering mixture of ZnO and Sb₂O₃ powders under 5 GPa at temperatures of 1100–1450 °C. The best *p*-type ZnO:Sb with resistivity of $1.6 \times 10^{-2} \Omega \text{ cm}$, carrier concentration of $3.3 \times 10^{20} \text{ cm}^{-3}$, and mobility of 12.1 cm²/V s was obtained by doping 4.6 at. % Sb and sintering at 1450 °C. The *p*-type conduction is due to complex acceptor formed by one substitutional Sb at Zn site and two Zn vacancies. The acceptor level was measured to be 113 meV. Effect of pressure on formation and electrical properties of the *p*-type ZnO:Sb is discussed. © 2009 American Institute of Physics. [DOI: 10.1063/1.3153515]

Due to a wide band gap of 3.37 eV and a large exciton binding energy of 60 meV at room temperature, ZnO has been considered as a promising semiconductor material for short-wavelength optoelectronic devices such as ultraviolet light emitting and laser diodes with low thresholds.^{1–3} However, difficulty in fabrication of stable and reproducible *p*-type ZnO with low resistivity and high carrier concentration hinders application of ZnO in optoelectronic field. The difficulty comes mainly from two factors: one is self-compensating effect from native defects such as oxygen vacancies (*V*_o) and interstitial zinc (*Zn*_i) (Ref. 4), and/or H incorporation,⁵ and the other is low solid solubility and deep acceptor level of acceptor dopants in ZnO, which lead to *p*-type ZnO having low hole concentration and high resistivity. Usually, the former is solved by improving ZnO crystal quality and the latter by doping in nonequilibrium thermodynamic state. However, the nonequilibrium doping is limited for improvement of doping content of the *p*-type dopant, moreover, it can make crystal quality poor and conductivity unstable. In addition, it is difficult to control growth process in nonequilibrium doping, resulting in that preparation of *p*-type ZnO is reproducible.

It is well known that high pressure can change the thermodynamic state of a system, which may increase solid solubility of a dopant in a system. Therefore, if *p*-type doping in ZnO is carried out under high pressure, solid solubility of a *p*-type dopant in ZnO may be increased, making electrical properties of the *p*-type ZnO improved. In addition, since the *p*-type doping under high pressure is performed in quasiequilibrium thermodynamic process, growth process of *p*-type ZnO can be controlled easily, leading to that preparation of *p*-type ZnO with good crystal quality is reproducible.

In recent years, V-group elements such as N, P, As, and Sb are used to fabricate *p*-type ZnO. Considering that Sb has similar ionic radius to Zn, Sb was selected as *p*-type dopant in the present work, and doped in ZnO under high pressure.

By doping under high pressure, it is expected to improve solid solubility of Sb in ZnO and preparation of stable and reproducible *p*-type ZnO with high carrier concentration and low resistivity.

In the present work, 99.99% pure ZnO powder and 99.99% pure Sb₂O₃ powder were mixed uniformly by various nominal mole ratios of the ZnO to Sb₂O₃, respectively. The mixture of the ZnO and Sb₂O₃ was pressed into a disk with diameter of 13 mm and height of 5 mm, and then put into a Mo ampoule to preventing from pollution. The Mo ampoule was encased into a graphite crucible used as a heater, which was encased in a pyrophyllite cube. A six-anvil high pressure apparatus, which can generate maximum pressure of 6 GPa, was employed for generating quasihydrostatic pressure using pyrophyllite as a pressure transmitting medium. Heating was performed by passing an electric current through the graphite crucible. The mixture was sintered isothermally for 15 min under 5 GPa in a temperature ranging from 800 to 2000 °C. Prior to various measurements, about 1 mm thick surface layer of the two sides of the as-sintered disk are removed to exclude possible effect induced by diffusion of Mo into the sample.

Hall measurement was performed for ZnO doped with nominal Sb content of 0–8.6 at. % and sintered for 15 min under 5 GPa at about 1100 °C, which indicates that the undoped ZnO is insulating and the ZnO doped with nominal Sb content of 1.4–8.6 at. % behave *p*-type conductivity with resistivity of 4.5×10^3 – $3.0 \times 10^{-1} \Omega \text{ cm}$ and carrier concentration of 3.5×10^{15} – $1.2 \times 10^{19} \text{ cm}^{-3}$. Moreover, the resistivity of the *p*-type ZnO decreases and the carrier concentration increases with increasing Sb content. Above results indicate that the *p*-type conduction of the Sb-doped ZnO is related to Sb doping and that the electrical properties of the *p*-type ZnO is improved with increasing Sb doping content. Table I shows Hall measurement results of ZnO doped with nominal Sb content of 8.6 at. % and sintered for 15 min under 5 GPa at temperatures of 800–2000 °C. The Sb-doped ZnO (denoted as ZnO:Sb) presents *n*-type conductivity as sintered at 800 °C, *p*-type conductivity as sintered at tem-

^{a)}Author to whom correspondence should be addressed. Electronic mail: yaobin196226@yahoo.com.cn.

TABLE I. Electrical properties of ZnO doped with nominal Sb content of 8.6 at. % and sintered under 5 GPa at various temperatures.

Temperature °C	Type	Resistivity Ω cm	Carrier concentration cm^{-3}	Mobility $\text{cm}^2 \text{V}^{-1} \text{s}^{-1}$
800	<i>n</i>	3.5×10^{-2}	1.4×10^{17}	1.6
1100	<i>p</i>	3.0×10^{-1}	1.3×10^{19}	2.6
1450	<i>p</i>	1.6×10^{-2}	3.3×10^{20}	12.1
2000	<i>n</i>	8.1×10^6	2.7×10^{10}	53.4

peratures between 1100 and 1450 °C, and high resistance as sintered at 2000 °C. The electrical properties of the ZnO:Sb depend on sintering temperature and the *p*-type conductivity is realized only in temperature region from 1100 to 1450 °C for ZnO doped with nominal 8.6 at. % Sb. The *p*-type ZnO:Sb obtained at 1450 °C shows the best electrical properties with resistivity of $1.6 \times 10^{-2} \Omega$ cm, carrier concentration of $3.3 \times 10^{20} \text{ cm}^{-3}$, and mobility of 12.1 $\text{cm}^2/\text{V s}$, which is better than electrical properties of the Sb-doped *p*-type ZnO reported previously.⁶⁻⁹ Keeping the *p*-type ZnO:Sb in air and making Hall measurement for it every one or two months, it is found that the *p*-type ZnO:Sb has behaved *p*-type conduction in a period of about 20 months since it was prepared, but its resistivity increases and carrier concentration decreases with increasing time. This implies that the *p*-type ZnO:Sb is of better stability. It is demonstrated experimentally that the *p*-type ZnO:Sb is reproducible and reproducibility is not smaller than 80%, which is attributed to that of the *p*-type doping performed in an equilibrium thermodynamic state.

Figures 1(a)–1(c) show x-ray diffraction (XRD) patterns of ZnO doped with nominal 8.6 at. % Sb and sintered at 800, 1100, and 1450 °C, respectively. Figure 1(a) shows that the Sb-doped ZnO sintered at 800 °C consists of ZnO:Sb, Sb, and an unknown phase I, implying that some Sb_2O_3 are deoxidized to Sb and some Sb_2O_3 react with ZnO to form the

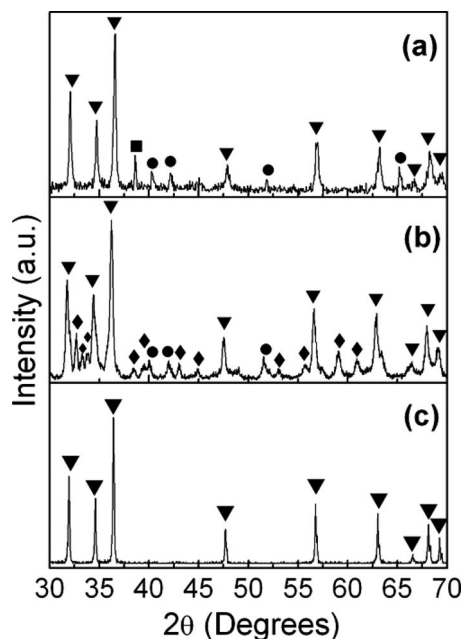


FIG. 1. XRD patterns of ZnO doped with nominal Sb content of 8.6 at. % and sintered under 5 GPa at (a) 800 °C, (b) 1100 °C, and (c) 1450 °C, respectively. ▼ ZnO:Sb, ● Sb ■ unknown phase I, ◆ unknown phase II.

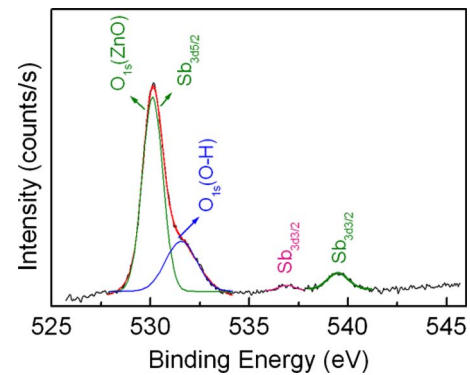


FIG. 2. (Color online) XPS of *p*-type ZnO doped with nominal Sb content of 8.6 at. % and sintered under 5 GPa at 1450 °C.

unknown phase I. When the Sb-doped ZnO is sintered at 1100 °C, it is concluded from Fig. 1(b) that the sample is composed by ZnO:Sb, Sb, and an unknown phase II. As the temperature rises to 1450 °C, as shown in Fig. 1(c), the Sb-doped ZnO consist only of ZnO:Sb phase, and no other phase is observed, implying that most of Sb incorporates into ZnO. Further increasing the temperature to 2000 °C, however, the sample consists of ZnO and Sb [XRD pattern and scanning electron microscopy (SEM) image are not shown here], and the Sb precipitates at grain boundaries and few Sb incorporates into ZnO. Above XRD results indicate that the Sb-doped ZnO obtained at 1450 °C has the highest Sb content.

Combining Hall results with XRD and SEM results, it is deduced that *p*-type conductivity of the Sb-doped ZnO is determined by Sb doping content, while presence of the other phases such as Sb and the unknown phases influence transport properties of the *p*-type ZnO:Sb, as shown in Table I, the mobility of the single phase sample produced at 1450 °C is much higher than that of multiphases samples produced at 1100 °C.

In order to understand the origin of the *p*-type conductivity, chemical environment, and content of Sb were studied by x-ray photoelectron spectroscopy (XPS) measurement for the *p*-type ZnO doped with nominal 8.6 at. % Sb and sintered at 1450 °C. As Fig. 2 shows, two $\text{Sb}_{3d3/2}$ bands are observed at binding energy of 536.9 and 539.5 eV, respectively. The 536.9 eV is close to binding energy of $\text{Sb}_{3d3/2}$ of metal Sb, and the 539.5 eV is near binding energy of $\text{Sb}_{3d3/2}$ of Sb–O bond. So it is deduced that the Sb has two kinds of chemical environments in the *p*-type ZnO:Sb, one is metal Sb, which locates at grain boundaries of the ZnO, and another substitutional Sb at Zn site (Sb_{Zn}). Based on Fig. 2, the Sb content is estimated to be 1.7 at. % in a form of Sb and 4.6 at. % in a form of Sb_{Zn} . Limpijumnon *et al.*¹⁰ proposed that Sb would substitute for Zn (Sb_{Zn}) instead of oxygen in the Sb-doped ZnO and then produce two corresponding Zn vacancies (V_{Zn}), which form a $\text{Sb}_{\text{Zn}}-2V_{\text{Zn}}$ complex acceptor. Therefore, the *p*-type conductivity of the ZnO:Sb comes mainly from contribution of the $\text{Sb}_{\text{Zn}}-2V_{\text{Zn}}$ complex in the present work.

It is known from literatures published previously that the highest Sb content is 2.3 at. % in ZnO film produced under vacuum, which is much less than the Sb content of 4.6 at. % obtained under high pressure. This implies that high pressure can improve solid solubility of Sb in ZnO. The good electri-

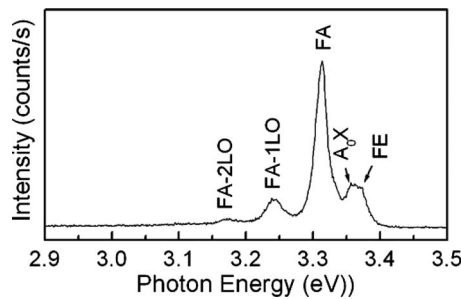


FIG. 3. 80 K PL spectrum of *p*-type ZnO doped with nominal Sb content of 8.6 at. % and sintered under 5 GPa at 1450 °C.

cal properties of the *p*-type ZnO:Sb may be related to the high Sb doping content.

In order to investigate optical properties and estimate $\text{Sb}_{\text{Zn}}-2V_{\text{Zn}}$ acceptor level, photoluminescence (PL) measurement is performed for the *p*-type ZnO doped with nominal 8.6 at. % Sb and sintered under 5 GPa at 1450 °C, as shown in Fig. 3. Five PL peaks are observed at 3.370, 3.359, 3.313, 3.241, and 3.170 eV, respectively. The 3.370, 3.359, and 3.313 eV peaks are ascribed to emission of free exciton, neutral acceptor bound exciton (A^0X), and electron transition from conduction band to acceptor level (FA), respectively. The 3.241 and 3.170 eV are due to first and second order longitudinal optical phonon replicas of the FA with a periodic spacing of ~ 72 meV. According to relationship between FA, acceptor level E_A , and bandgap E_g , $FA = E_g - E_A + k_B T/2$, the E_A is estimated to 113 meV above valence band maximum, less than acceptor levels reported previously.^{6–9} Semiconductor theory indicates that heavy doping can lead to decrease in acceptor level. So, the low E_A may be related to the high Sb doping content in ZnO.

In summary, stable *p*-type ZnO:Sb was fabricated reproducibly by doping nominal Sb content from 1.4 to 8.6 at. % and sintering under 5 GPa at temperatures of 1100–1450 °C. The best *p*-type ZnO:Sb with resistivity of $1.6 \times 10^{-2} \Omega \text{ cm}$, carrier concentration of $3.3 \times 10^{20} \text{ cm}^{-3}$, and mobility of 12.08 cm^2/Vs was obtained by doping 4.6 at. % Sb and sintering at 1450 °C, and has shown *p*-type conductivity in a period of 20 months up to now. The *p*-type conduction comes from contribution of $\text{Sb}_{\text{Zn}}-2V_{\text{Zn}}$ complex acceptor, which is of acceptor level of 113 meV above valence band maximum.

This work is supported by National Natural Science Foundation of China under Grant No. 50532050, 6077601, 60506014, 10674133, 60806002, and 10874178; the “973” program under Grant No. 2006CB604906; and Scientific and Technological Development Project of Jilin Province under Grant No. 20080510.

¹S. Choopun, R. D. Vispute, W. Noch, A. Balsamo, R. P. Sharma, T. Venkatesan, A. Iliadis, and D. C. Look, *Appl. Phys. Lett.* **75**, 3947 (1999).

²E. M. Wong and P. C. Searson, *Appl. Phys. Lett.* **74**, 2939 (1999).

³H. J. Ko, Y. F. Chen, Z. Zhu, T. Yao, I. Kobayashi, and H. Uchiki, *Appl. Phys. Lett.* **76**, 1905 (2000).

⁴S. B. Zhang, S. H. Wei, and A. Zunger, *Phys. Rev. B* **63**, 075205 (2001).

⁵C. G. Van de Walle, *Phys. Rev. Lett.* **85**, 1012 (2000).

⁶F. X. Xiu, Z. Yang, L. J. Mandalapu, D. T. Zhao, J. L. Liu, and W. P. Beyermann, *Appl. Phys. Lett.* **87**, 152101 (2005).

⁷E. Przeździecka, E. Kamińska, I. Pasternak, A. Piotrowska, and J. Kossut, *Phys. Rev. B* **76**, 193303 (2007).

⁸X. H. Pan, Z. Z. Ye, H. S. Li, Y. J. Zeng, X. Q. Gu, L. P. Zhu, B. H. Zhao, and Y. Che, *Appl. Surf. Sci.* **253**, 5067 (2007).

⁹T. Aoki, Y. Shimizu, A. Miyake, A. Nakamura, Y. Nakanishi, and Y. Hatanaka, *Phys. Status Solidi B* **229**, 911 (2002).

¹⁰S. Limpijumnong, S. B. Zhang, S. H. Wei, and C. H. Park, *Phys. Rev. Lett.* **92**, 155504 (2004).